# Observation and polarization measurement of $B^0 \to a_1(1260)^+ a_1(1260)^-$ decay

B. Aubert,[1] Y. Karyotakis,[1] J. P. Lees,[1] V. Poireau,[1] E. Prencipe,[1] X. Prudent,[1] V. Tisserand,[1] J. Garra Tico,[2] E. Grauges,[2] M. Martinelli,[3a,3b] A. Palano,[3a,3b] M. Pappagallo,[3a,3b] G. Eigen,[4] B. Stugu,[4] L. Sun,[4] M. Battaglia,[5] D. N. Brown,[5] L. T. Kerth,[5] Yu. G. Kolomensky,[5] G. Lynch,[5] I. L. Osipenkov,[5] K. Tackmann,[5] T. Tanabe,[5] C. M. Hawkes,[6] N. Soni,[6] A. T. Watson,[6] H. Koch,[7] T. Schroeder,[7] D. J. Asgeirsson,[8] B. G. Fulsom,[8] C. Hearty,[8] T. S. Mattison,[8] J. A. McKenna,[8] M. Barrett,[9] A. Khan,[9] A. Randle-Conde,[9] V. E. Blinov,[10] A. D. Bukin,[10,*] A. R. Buzykaev,[10] V. P. Druzhinin,[10] V. B. Golubev,[10] A. P. Onuchin,[10] S. I. Serednyakov,[10] Yu. I. Skovpen,[10] E. P. Solodov,[10] K. Yu. Todyshev,[10] M. Bondioli,[11] S. Curry,[11] I. Eschrich,[11] D. Kirkby,[11] A. J. Lankford,[11] P. Lund,[11] M. Mandelkern,[11] E. C. Martin,[11] D. P. Stoker,[11] H. Atmacan,[12] J. W. Gary,[12] F. Liu,[12] O. Long,[12] G. M. Vitug,[12] Z. Yasin,[12] V. Sharma,[13] C. Campagnari,[14] T. M. Hong,[14] D. Kovalskyi,[14] M. A. Mazur,[14] J. D. Richman,[14] T. W. Beck,[15] A. M. Eisner,[15] C. A. Heusch,[15] J. Kroseberg,[15] W. S. Lockman,[15] A. J. Martinez,[15] T. Schalk,[15] B. A. Schumm,[15] A. Seiden,[15] L. Wang,[15] L. O. Winstrom,[15] C. H. Cheng,[16] D. A. Doll,[16] B. Echenard,[16] F. Fang,[16] D. G. Hitlin,[16] I. Narsky,[16] P. Ongmongkolkul,[16] T. Piatenko,[16] F. C. Porter,[16] R. Andreassen,[17] G. Mancinelli,[17] B. T. Meadows,[17] K. Mishra,[17] M. D. Sokoloff,[17] P. C. Bloom,[18] W. T. Ford,[18] A. Gaz,[18] J. F. Hirschauer,[18] M. Nagel,[18] U. Nauenberg,[18] J. G. Smith,[18] S. R. Wagner,[18] R. Ayad,[19,†] W. H. Toki,[19] R. J. Wilson,[19] E. Feltresi,[20] A. Hauke,[20] H. Jasper,[20] T. M. Karbach,[20] J. Merkel,[20] A. Petzold,[20] B. Spaan,[20] K. Wacker,[20] M. J. Kobel,[21] R. Nogowski,[21] K. R. Schubert,[21] R. Schwierz,[21] A. Volk,[21] D. Bernard,[22] E. Latour,[22] M. Verderi,[22] P. J. Clark,[23] S. Playfer,[23] J. E. Watson,[23] M. Andreotti,[24a,24b] D. Bettoni,[24a] C. Bozzi,[24a] R. Calabrese,[24a,24b] A. Cecchi,[24a,24b] G. Cibinetto,[24a,24b] E. Fioravanti,[24a,24b] P. Franchini,[24a,24b] E. Luppi,[24a,24b] M. Munerato,[24a,24b] M. Negrini,[24a,24b] A. Petrella,[24a,24b] L. Piemontese,[24a] V. Santoro,[24a,24b] R. Baldini-Ferroli,[25] A. Calcaterra,[25] R. de Sangro,[25] G. Finocchiaro,[25] S. Pacetti,[25] P. Patteri,[25] I. M. Peruzzi,[25,‡] M. Piccolo,[25] M. Rama,[25] A. Zallo,[25] R. Contri,[26a,26b] E. Guido,[26a] M. Lo Vetere,[26a,26b] M. R. Monge,[26a,26b] S. Passaggio,[26a] C. Patrignani,[26a,26b] E. Robutti,[26a] S. Tosi,[26a,26b] K. S. Chaisanguanthum,[27] M. Morii,[27] A. Adametz,[28] J. Marks,[28] S. Schenk,[28] U. Uwer,[28] F. U. Bernlochner,[29] V. Klose,[29] H. M. Lacker,[29] D. J. Bard,[30] P. D. Dauncey,[30] M. Tibbetts,[30] P. K. Behera,[31] M. J. Charles,[31] U. Mallik,[31] J. Cochran,[32] H. B. Crawley,[32] L. Dong,[32] V. Eyges,[32] W. T. Meyer,[32] S. Prell,[32] E. I. Rosenberg,[32] A. E. Rubin,[32] Y. Y. Gao,[33] A. V. Gritsan,[33] Z. J. Guo,[33] N. Arnaud,[34] J. Béquilleux,[34] A. D'Orazio,[34] M. Davier,[34] D. Derkach,[34] J. Firmino da Costa,[34] G. Grosdidier,[34] F. Le Diberder,[34] V. Lepeltier,[34] A. M. Lutz,[34] B. Malaescu,[34] S. Pruvot,[34] P. Roudeau,[34] M. H. Schune,[34] J. Serrano,[34] V. Sordini,[34,§] A. Stocchi,[34] G. Wormser,[34] D. J. Lange,[35] D. M. Wright,[35] I. Bingham,[36] J. P. Burke,[36] C. A. Chavez,[36] J. R. Fry,[36] E. Gabathuler,[36] R. Gamet,[36] D. E. Hutchcroft,[36] D. J. Payne,[36] C. Touramanis,[36] A. J. Bevan,[37] C. K. Clarke,[37] F. Di Lodovico,[37] R. Sacco,[37] M. Sigamani,[37] G. Cowan,[38] S. Paramesvaran,[38] A. C. Wren,[38] D. N. Brown,[39] C. L. Davis,[39] A. G. Denig,[40] M. Fritsch,[40] W. Gradl,[40] A. Hafner,[40] K. E. Alwyn,[41] D. Bailey,[41] R. J. Barlow,[41] G. Jackson,[41] G. D. Lafferty,[41] T. J. West,[41] J. I. Yi,[41] J. Anderson,[42] C. Chen,[42] A. Jawahery,[42] D. A. Roberts,[42] G. Simi,[42] J. M. Tuggle,[42] C. Dallapiccola,[43] E. Salvati,[43] R. Cowan,[44] D. Dujmic,[44] P. H. Fisher,[44] S. W. Henderson,[44] G. Sciolla,[44] M. Spitznagel,[44] R. K. Yamamoto,[44] M. Zhao,[44] P. M. Patel,[45] S. H. Robertson,[45] M. Schram,[45] P. Biassoni,[46a,46b] P. Gandini,[46a,46b] A. Lazzaro,[46a,46b] V. Lombardo,[46a] F. Palombo,[46a,46b] S. Stracka,[46a,46b] J. M. Bauer,[47] L. Cremaldi,[47] R. Godang,[47,‖] R. Kroeger,[47] P. Sonnek,[47] D. J. Summers,[47] H. W. Zhao,[47] M. Simard,[48] P. Taras,[48] H. Nicholson,[49] G. De Nardo,[50a,50b] L. Lista,[50a] D. Monorchio,[50a,50b] G. Onorato,[50a,50b] C. Sciacca,[50a,50b] G. Raven,[51] H. L. Snoek,[51] C. P. Jessop,[52] K. J. Knoepfel,[52] J. M. LoSecco,[52] W. F. Wang,[52] L. A. Corwin,[53] K. Honscheid,[53] H. Kagan,[53] R. Kass,[53] J. P. Morris,[53] A. M. Rahimi,[53] J. J. Regensburger,[53] S. J. Sekula,[53] Q. K. Wong,[53] N. L. Blount,[54] J. Brau,[54] R. Frey,[54] O. Igonkina,[54] J. A. Kolb,[54] M. Lu,[54] R. Rahmat,[54] N. B. Sinev,[54] D. Strom,[54] J. Strube,[54] E. Torrence,[54] G. Castelli,[55a,55b] N. Gagliardi,[55a,55b] M. Margoni,[55a,55b] M. Morandin,[55a] M. Posocco,[55a] M. Rotondo,[55a] F. Simonetto,[55a,55b] R. Stroili,[55a,55b] C. Voci,[55a,55b] P. del Amo Sanchez,[56] E. Ben-Haim,[56] G. R. Bonneaud,[56] H. Briand,[56] J. Chauveau,[56] O. Hamon,[56] Ph. Leruste,[56] G. Marchiori,[56] J. Ocariz,[56] A. Perez,[56] J. Prendki,[56] S. Sitt,[56] L. Gladney,[57] M. Biasini,[58a,58b] E. Manoni,[58a,58b] C. Angelini,[59a,59b] G. Batignani,[59a,59b] S. Bettarini,[59a,59b] G. Calderini,[59a,59b,¶] M. Carpinelli,[59a,59b,**] A. Cervelli,[59a,59b] F. Forti,[59a,59b] M. A. Giorgi,[59a,59b] A. Lusiani,[59a,59c] M. Morganti,[59a,59b] N. Neri,[59a,59b] E. Paoloni,[59a,59b] G. Rizzo,[59a,59b] J. J. Walsh,[59a] D. Lopes Pegna,[60] C. Lu,[60] J. Olsen,[60] A. J. S. Smith,[60] A. V. Telnov,[60] F. Anulli,[61a] E. Baracchini,[61a,61b] G. Cavoto,[61a] R. Faccini,[61a,61b] F. Ferrarotto,[61a] F. Ferroni,[61a,61b] M. Gaspero,[61a,61b] P. D. Jackson,[61a] L. Li Gioi,[61a] M. A. Mazzoni,[61a] S. Morganti,[61a] G. Piredda,[61a] F. Renga,[61a,61b] C. Voena,[61a] M. Ebert,[62] T. Hartmann,[62] H. Schröder,[62] R. Waldi,[62] T. Adye,[63] B. Franek,[63] E. O. Olaiya,[63] F. F. Wilson,[63] S. Emery,[64] L. Esteve,[64] G. Hamel de Monchenault,[64] W. Kozanecki,[64] G. Vasseur,[64] Ch. Yèche,[64] M. Zito,[64] M. T. Allen,[65] D. Aston,[65] R. Bartoldus,[65] J. F. Benitez,[65]

 

R. Cenci,[65] J. P. Coleman,[65] M. R. Convery,[65] J. C. Dingfelder,[65] J. Dorfan,[65] G. P. Dubois-Felsmann,[65] W. Dunwoodie,[65] R. C. Field,[65] M. Franco Sevilla,[65] A. M. Gabareen,[65] M. T. Graham,[65] P. Grenier,[65] C. Hast,[65] W. R. Innes,[65] J. Kaminski,[65] M. H. Kelsey,[65] H. Kim,[65] P. Kim,[65] M. L. Kocian,[65] D. W. G. S. Leith,[65] S. Li,[65] B. Lindquist,[65] S. Luitz,[65] V. Luth,[65] H. L. Lynch,[65] D. B. MacFarlane,[65] H. Marsiske,[65] R. Messner,[65,*] D. R. Muller,[65] H. Neal,[65] S. Nelson,[65] C. P. O'Grady,[65] I. Ofte,[65] M. Perl,[65] B. N. Ratcliff,[65] A. Roodman,[65] A. A. Salnikov,[65] R. H. Schindler,[65] J. Schwiening,[65] A. Snyder,[65] D. Su,[65] M. K. Sullivan,[65] K. Suzuki,[65] S. K. Swain,[65] J. M. Thompson,[65] J. Va'vra,[65] A. P. Wagner,[65] M. Weaver,[65] C. A. West,[65] W. J. Wisniewski,[65] M. Wittgen,[65] D. H. Wright,[65] H. W. Wulsin,[65] A. K. Yarritu,[65] C. C. Young,[65] V. Ziegler,[65] X. R. Chen,[66] H. Liu,[66] W. Park,[66] M. V. Purohit,[66] R. M. White,[66] J. R. Wilson,[66] P. R. Burchat,[67] A. J. Edwards,[67] T. S. Miyashita,[67] S. Ahmed,[68] M. S. Alam,[68] J. A. Ernst,[68] B. Pan,[68] M. A. Saeed,[68] S. B. Zain,[68] A. Soffer,[69] S. M. Spanier,[70] B. J. Wogsland,[70] R. Eckmann,[71] J. L. Ritchie,[71] A. M. Ruland,[71] C. J. Schilling,[71] R. F. Schwitters,[71] B. C. Wray,[71] B. W. Drummond,[72] J. M. Izen,[72] X. C. Lou,[72] F. Bianchi,[73a,73b] D. Gamba,[73a,73b] M. Pelliccioni,[73a,73b] M. Bomben,[74a,74b] L. Bosisio,[74a,74b] C. Cartaro,[74a,74b] G. Della Ricca,[74a,74b] L. Lanceri,[74a,74b] L. Vitale,[74a,74b] V. Azzolini,[75] N. Lopez-March,[75] F. Martinez-Vidal,[75] D. A. Milanes,[75] A. Oyanguren,[75] J. Albert,[76] Sw. Banerjee,[76] B. Bhuyan,[76] H. H. F. Choi,[76] K. Hamano,[76] G. J. King,[76] R. Kowalewski,[76] M. J. Lewczuk,[76] I. M. Nugent,[76] J. M. Roney,[76] R. J. Sobie,[76] T. J. Gershon,[77] P. F. Harrison,[77] J. Ilic,[77] T. E. Latham,[77] G. B. Mohanty,[77] E. M. T. Puccio,[77] H. R. Band,[78] X. Chen,[78] S. Dasu,[78] K. T. Flood,[78] Y. Pan,[78] R. Prepost,[78] C. O. Vuosalo,[78] and S. L. Wu[78]

(*BABAR* Collaboration)

[1]*Laboratoire d'Annecy-le-Vieux de Physique des Particules (LAPP), Université de Savoie, CNRS/IN2P3, F-74941 Annecy-Le-Vieux, France*
[2]*Universitat de Barcelona, Facultat de Fisica, Departament ECM, E-08028 Barcelona, Spain*
[3a]*INFN Sezione di Bari, I-70126 Bari, Italy*
[3b]*Dipartimento di Fisica, Università di Bari, I-70126 Bari, Italy*
[4]*University of Bergen, Institute of Physics, N-5007 Bergen, Norway*
[5]*Lawrence Berkeley National Laboratory and University of California, Berkeley, California 94720, USA*
[6]*University of Birmingham, Birmingham, B15 2TT, United Kingdom*
[7]*Ruhr Universität Bochum, Institut für Experimentalphysik 1, D-44780 Bochum, Germany*
[8]*University of British Columbia, Vancouver, British Columbia, Canada V6T 1Z1*
[9]*Brunel University, Uxbridge, Middlesex UB8 3PH, United Kingdom*
[10]*Budker Institute of Nuclear Physics, Novosibirsk 630090, Russia*
[11]*University of California at Irvine, Irvine, California 92697, USA*
[12]*University of California at Riverside, Riverside, California 92521, USA*
[13]*University of California at San Diego, La Jolla, California 92093, USA*
[14]*University of California at Santa Barbara, Santa Barbara, California 93106, USA*
[15]*University of California at Santa Cruz, Institute for Particle Physics, Santa Cruz, California 95064, USA*
[16]*California Institute of Technology, Pasadena, California 91125, USA*
[17]*University of Cincinnati, Cincinnati, Ohio 45221, USA*
[18]*University of Colorado, Boulder, Colorado 80309, USA*
[19]*Colorado State University, Fort Collins, Colorado 80523, USA*
[20]*Technische Universität Dortmund, Fakultät Physik, D-44221 Dortmund, Germany*
[21]*Technische Universität Dresden, Institut für Kern-und Teilchenphysik, D-01062 Dresden, Germany*
[22]*Laboratoire Leprince-Ringuet, CNRS/IN2P3, Ecole Polytechnique, F-91128 Palaiseau, France*
[23]*University of Edinburgh, Edinburgh EH9 3JZ, United Kingdom*
[24a]*INFN Sezione di Ferrara, I-44100 Ferrara, Italy*
[24b]*Dipartimento di Fisica, Università di Ferrara, I-44100 Ferrara, Italy*
[25]*INFN Laboratori Nazionali di Frascati, I-00044 Frascati, Italy*
[26a]*INFN Sezione di Genova, I-16146 Genova, Italy*
[26b]*Dipartimento di Fisica, Università di Genova, I-16146 Genova, Italy*
[27]*Harvard University, Cambridge, Massachusetts 02138, USA*
[28]*Universität Heidelberg, Physikalisches Institut, Philosophenweg 12, D-69120 Heidelberg, Germany*
[29]*Humboldt-Universität zu Berlin, Institut für Physik, Newtonstr. 15, D-12489 Berlin, Germany*
[30]*Imperial College London, London, SW7 2AZ, United Kingdom*
[31]*University of Iowa, Iowa City, Iowa 52242, USA*
[32]*Iowa State University, Ames, Iowa 50011-3160, USA*
[33]*Johns Hopkins University, Baltimore, Maryland 21218, USA*

[34]Laboratoire de l'Accélérateur Linéaire, IN2P3/CNRS et Université Paris-Sud 11, Centre Scientifique d'Orsay, B. P. 34, F-91898 Orsay Cedex, France
[35]Lawrence Livermore National Laboratory, Livermore, California 94550, USA
[36]University of Liverpool, Liverpool L69 7ZE, United Kingdom
[37]Queen Mary, University of London, London, E1 4NS, United Kingdom
[38]University of London, Royal Holloway and Bedford New College, Egham, Surrey TW20 0EX, United Kingdom
[39]University of Louisville, Louisville, Kentucky 40292, USA
[40]Johannes Gutenberg-Universität Mainz, Institut für Kernphysik, D-55099 Mainz, Germany
[41]University of Manchester, Manchester M13 9PL, United Kingdom
[42]University of Maryland, College Park, Maryland 20742, USA
[43]University of Massachusetts, Amherst, Massachusetts 01003, USA
[44]Massachusetts Institute of Technology, Laboratory for Nuclear Science, Cambridge, Massachusetts 02139, USA
[45]McGill University, Montréal, Québec, Canada H3A 2T8
[46a]INFN Sezione di Milano, I-20133 Milano, Italy
[46b]Dipartimento di Fisica, Università di Milano, I-20133 Milano, Italy
[47]University of Mississippi, University, Mississippi 38677, USA
[48]Université de Montréal, Physique des Particules, Montréal, Québec, Canada H3C 3J7
[49]Mount Holyoke College, South Hadley, Massachusetts 01075, USA
[50a]INFN Sezione di Napoli, I-80126 Napoli, Italy
[50b]Dipartimento di Scienze Fisiche, Università di Napoli Federico II, I-80126 Napoli, Italy
[51]NIKHEF, National Institute for Nuclear Physics and High Energy Physics, NL-1009 DB Amsterdam, The Netherlands
[52]University of Notre Dame, Notre Dame, Indiana 46556, USA
[53]Ohio State University, Columbus, Ohio 43210, USA
[54]University of Oregon, Eugene, Oregon 97403, USA
[55a]INFN Sezione di Padova, I-35131 Padova, Italy
[55b]Dipartimento di Fisica, Università di Padova, I-35131 Padova, Italy
[56]Laboratoire de Physique Nucléaire et de Hautes Energies, IN2P3/CNRS, Université Pierre et Marie Curie-Paris6, Université Denis Diderot-Paris7, F-75252 Paris, France
[57]University of Pennsylvania, Philadelphia, Pennsylvania 19104, USA
[58a]INFN Sezione di Perugia, I-06100 Perugia, Italy
[58b]Dipartimento di Fisica, Università di Perugia, I-06100 Perugia, Italy
[59a]INFN Sezione di Pisa, I-56127 Pisa, Italy
[59b]Dipartimento di Fisica, Università di Pisa, I-56127 Pisa, Italy
[59c]Scuola Normale Superiore di Pisa, I-56127 Pisa, Italy
[60]Princeton University, Princeton, New Jersey 08544, USA
[61a]INFN Sezione di Roma, I-00185 Roma, Italy
[61b]Dipartimento di Fisica, Università di Roma La Sapienza, I-00185 Roma, Italy
[62]Universität Rostock, D-18051 Rostock, Germany
[63]Rutherford Appleton Laboratory, Chilton, Didcot, Oxon, OX11 0QX, United Kingdom
[64]CEA, Irfu, SPP, Centre de Saclay, F-91191 Gif-sur-Yvette, France
[65]SLAC National Accelerator Laboratory, Stanford, California 94309 USA
[66]University of South Carolina, Columbia, South Carolina 29208, USA
[67]Stanford University, Stanford, California 94305-4060, USA
[68]State University of New York, Albany, New York 12222, USA
[69]Tel Aviv University, School of Physics and Astronomy, Tel Aviv, 69978, Israel
[70]University of Tennessee, Knoxville, Tennessee 37996, USA
[71]University of Texas at Austin, Austin, Texas 78712, USA
[72]University of Texas at Dallas, Richardson, Texas 75083, USA
[73a]INFN Sezione di Torino, I-10125 Torino, Italy
[73b]Dipartimento di Fisica Sperimentale, Università di Torino, I-10125 Torino, Italy
[74a]INFN Sezione di Trieste, I-34127 Trieste, Italy
[74b]Dipartimento di Fisica, Università di Trieste, I-34127 Trieste, Italy
[75]IFIC, Universitat de Valencia-CSIC, E-46071 Valencia, Spain

[*]Deceased.
[†]Now at Temple University, Philadelphia, PA 19122, USA.
[‡]Also with Università di Perugia, Dipartimento di Fisica, Perugia, Italy.
[§]Also with Università di Roma La Sapienza, I-00185 Roma, Italy.
[‖]Now at University of South Alabama, Mobile, AL 36688, USA.
[¶]Also with Laboratoire de Physique Nucléaire et de Hautes Energies, IN2P3/CNRS, Université Pierre et Marie Curie-Paris6, Université Denis Diderot-Paris7, F-75252 Paris, France.
[**]Also with Università di Sassari, Sassari, Italy.

[76]*University of Victoria, Victoria, British Columbia, Canada V8W 3P6*
[77]*Department of Physics, University of Warwick, Coventry CV4 7AL, United Kingdom*
[78]*University of Wisconsin, Madison, Wisconsin 53706, USA*
(Received 13 July 2009; published 20 November 2009)

We present measurements of the branching fraction $\mathcal{B}$ and longitudinal polarization fraction $f_L$ for $B^0 \to a_1(1260)^+ a_1(1260)^-$ decays, with $a_1(1260)^\pm \to \pi^-\pi^+\pi^\pm$. The data sample, collected with the *BABAR* detector at the SLAC National Accelerator Laboratory, represents $465 \times 10^6$ produced $B\bar{B}$ pairs. We measure $\mathcal{B}(B^0 \to a_1(1260)^+ a_1(1260)^-) \times [\mathcal{B}(a_1(1260)^+ \to \pi^-\pi^+\pi^+)]^2 = (11.8 \pm 2.6 \pm 1.6) \times 10^{-6}$ and $f_L = 0.31 \pm 0.22 \pm 0.10$, where the first uncertainty is statistical and the second systematic. The decay mode is measured with a significance of 5.0 standard deviations including systematic uncertainties.

DOI: 10.1103/PhysRevD.80.092007 PACS numbers: 13.25.Hw, 11.30.Er, 12.15.Hh

Charmless $B$ decays to final states involving two axial-vector mesons ($AA$) have received considerable theoretical attention in the last few years [1–3]. The branching fractions of several $B \to AA$ decay modes have been calculated using the QCD factorization [2] and the naive factorization [3] approaches. Theoretical predictions for the branching fraction of the $B^0 \to a_1(1260)^+ a_1(1260)^-$ decay mode vary between $37.4 \times 10^{-6}$ [2] and $6.4 \times 10^{-6}$ [3]. Branching fractions at this level should be observable with the *BABAR* data sample, which can be used to discriminate between the predictions. The only available experimental information on this $B$ decay mode is the branching fraction upper limit of $2.8 \times 10^{-3}$ at 90% confidence level measured by CLEO [4].

The study of the decay polarization in the charmless $B$ decays to vector vector ($VV$), vector axial-vector ($VA$), and $AA$ mesons provides information on the underlying helicity structure of the decay mechanism [2]. The measured value of the longitudinal polarization fraction $f_L \sim 0.5$ in penguin-dominated $B \to \phi K^*$ decays [5] is in contrast with naive standard model (SM) calculations predicting a dominant longitudinal polarization ($f_L \sim 1$) [6]. The naive SM expectation is confirmed in the tree-dominated $B \to \rho\rho$ [7] and $B^+ \to \omega\rho^+$ [8] decays. A value of $f_L \sim 1$ is found in vector-tensor $B \to \phi K_2^*(1430)$ decays [9], while $f_L \sim 0.5$ is found in $B \to \omega K_2^*(1430)$ decays [8]. The small value of $f_L$ observed in $B \to \phi K^*$ decays has stimulated theoretical effort, such as the introduction of non-factorizable terms and penguin-annihilation amplitudes [10]. Other explanations invoke new physics [11].

There are no experimental measurements of $f_L$ in $B \to AA$ decays. The predicted value of the $f_L$ in $B^0 \to a_1^+ a_1^-$ [12] is 0.64 [2].

We present the first measurements of the branching fraction and polarization in $B^0 \to a_1^+ a_1^-$ decays, with $a_1^+ \to \pi^-\pi^+\pi^+$ [13]. We do not separate the $P$-wave $(\pi\pi)_\rho$ and the $S$-wave $(\pi\pi)_\sigma$ components in the $a_1 \to 3\pi$ decay; a systematic uncertainty is estimated due to the difference in the selection efficiencies [14]. Because of the limited number of signal events expected in the data sample, we do not perform a full angular analysis. Using helicity formalism, and after integration over the azimuthal angle between the decay planes of the two $a_1$ mesons, the predicted angular distribution $d\Gamma/d\cos\theta$ is

$$\frac{1}{\Gamma}\frac{d\Gamma}{d\cos\theta} \propto f_L(1-\cos^2\theta) + \frac{1}{2}f_T(1+\cos^2\theta), \quad (1)$$

where $f_T = 1 - f_L$ and $\theta$ is the angle between the normal to the decay plane of the three pions of one $a_1$ and the flight direction of the other $a_1$, both calculated in the rest frame of the first $a_1$.

The results presented here are based on data collected with the *BABAR* detector [15] at the PEP-II asymmetric-energy $e^+e^-$ collider [16] located at the SLAC National Accelerator Laboratory. The analysis uses an integrated luminosity of 423.0 fb$^{-1}$, corresponding to $(465 \pm 5) \times 10^6$ $B\bar{B}$ pairs, recorded at the $\Upsilon(4S)$ resonance at a center-of-mass energy of $\sqrt{s} = 10.58$ GeV. An additional 43.9 fb$^{-1}$, taken about 40 MeV below this energy (off-resonance data), is used for the study of the $q\bar{q}$ continuum background ($e^+e^- \to q\bar{q}$, with $q = u, d, s, c$).

Charged particles are detected, and their momenta measured, by a combination of a vertex tracker consisting of five layers of double-sided silicon microstrip detectors, and a 40-layer central drift chamber, both operating in the 1.5 T magnetic field of a superconducting solenoid. The tracking system covers 92% of the solid angle in the center-of-mass frame. We identify photons and electrons using a CsI(Tl) electromagnetic calorimeter. Further charged-particle identification is provided by the specific energy loss ($dE/dx$) in the tracking devices and by an internally reflecting ring-imaging Cherenkov detector covering the central region. A $K/\pi$ separation of better than 4 standard deviations is achieved for momenta below 3 GeV/$c$, decreasing to $2.5\sigma$ at the highest momenta in the $B$ decay final states. A more detailed description of the reconstruction of charged tracks in *BABAR* can be found elsewhere [17].

Monte Carlo (MC) simulations of the signal decay mode, continuum, $B\bar{B}$ backgrounds, and detector response [18] are used to establish the event selection criteria. The MC signal events are simulated as $B^0$ decays to $a_1^+ a_1^-$ with

$a_1 \to \rho(770)\pi$. The $a_1$ meson parameters in the simulation are mass $m_0 = 1230\ \mathrm{MeV}/c^2$ and width $\Gamma_0 = 400\ \mathrm{MeV}/c^2$ [19,20].

We reconstruct the decay of $a_1^+$ into three charged pions. Two pion candidates are combined to form a $\rho^0$ candidate. Candidates with an invariant mass between 0.51 and 1.10 $\mathrm{GeV}/c^2$ are combined with a third pion to form an $a_1$ candidate. The $a_1$ candidate is required to have a mass between 0.87 and 1.75 $\mathrm{GeV}/c^2$. We impose several particle identification requirements to ensure the identity of the signal pions. We also require the $\chi^2$ probability of the $B$ vertex fit to be greater than 0.01 and the number of charged tracks in the event to be greater or equal to seven.

A $B$ meson candidate is kinematically characterized by the energy-substituted mass $m_{\mathrm{ES}} \equiv \sqrt{(s/2 + \mathbf{p}_0 \cdot \mathbf{p}_B)^2/E_0^2 - \mathbf{p}_B^2}$ and energy difference $\Delta E \equiv E_B^* - \sqrt{s}/2$, where the subscripts 0 and $B$ refer to the initial $\Upsilon(4S)$ and the $B$ candidate in the laboratory frame, respectively, and the asterisk denotes the $\Upsilon(4S)$ frame. The resolutions in $m_{\mathrm{ES}}$ and $\Delta E$ are about 3.0 $\mathrm{MeV}/c^2$ and 20 MeV, respectively. We require candidates to satisfy $5.27 \le m_{\mathrm{ES}} \le 5.29\ \mathrm{GeV}/c^2$ and $-90 < \Delta E < 70$ MeV.

Background arises primarily from random track combinations in continuum events. We reduce this background by using the angle $\theta_T$ between the thrust axis of the $B$ candidate and the thrust axis of the rest of the event, evaluated in the $\Upsilon(4S)$ rest frame. The distribution of $|\cos\theta_T|$ is sharply peaked near 1 for combinations drawn from jetlike continuum events and is nearly uniform for $B\bar{B}$ events; for this reason, we require $|\cos\theta_T| < 0.65$.

Background can also arise from $B\bar{B}$ events, especially events containing a charmed meson (these are mostly events with five pions and a misidentified kaon in the final state). The charmed background includes peaking modes, with structures in $m_{\mathrm{ES}}$ and $\Delta E$ that mimic signal events, and nonpeaking "generic" modes. To suppress the charm background, we reconstruct $D$ and $D^*$ mesons. Events are vetoed if they contain $D$ or $D^*$ candidates with reconstructed masses within 20 $\mathrm{MeV}/c^2$ (window size of about $\pm 2\sigma$) of the nominal charmed meson masses [19].

The mean number of $B$ candidates per event is 2.9. If an event has multiple $B$ candidates, we select the candidate with the highest $B$ vertex $\chi^2$ probability. From MC simulation, we find that this algorithm selects the correct candidate 90% of the time in signal events while inducing negligible bias.

Using MC simulation of signal events with longitudinal (transverse) polarization, signal events are divided in two categories: correctly reconstructed signal (CR), where all candidate particles come from the correct signal $B^0$, and self-cross feed (SCF) signal, where candidate particles are exchanged with a rest of the event particle. The fraction of SCF candidates is $31.8 \pm 3.2(19.4 \pm 1.9)\%$.

We determine the number of signal events (the signal yield) from an unbinned extended maximum-likelihood fit. The seven input observables are $\Delta E$, $m_{\mathrm{ES}}$, a Fisher discriminant $\mathcal{F}$ [17], the two $a_1$ masses, and the two $\mathcal{H} = |\cos\theta|$. The Fisher discriminant $\mathcal{F}$ combines four variables calculated in the $\Upsilon(4S)$ frame: the absolute values of the cosines of the angles with respect to the beam axis of the $B$ momentum and the thrust axis of the $B$ decay products, and the zeroth and second angular Legendre moments $L_{0,2}$ of the momentum flow about the $B$ thrust axis. The Legendre moments are defined by $L_k = \sum_m p_m |\cos\theta_m|^k$, where $\theta_m$ is the angle with respect to the $B$ thrust axis of a track or neutral cluster $m$, $p_m$ is its momentum, and the sum includes the rest of the event particles only.

There are five hypotheses in the likelihood model: signal, continuum, and three $B\bar{B}$ components, which take into account charmless, generic charm, and peaking charm backgrounds. The likelihood function is

$$\mathcal{L} = e^{-(\sum_{j=1}^{5} n_j)} \prod_{i=1}^{N} \Big[ \sum_{j=1}^{5} n_j \mathcal{P}_j(\mathbf{x}_i) \Big], \tag{2}$$

where $N$ is the number of input events, $n_j$ is the number of events for hypothesis $j$, and $\mathcal{P}_j(\mathbf{x}_i)$ is the corresponding probability density function (PDF), evaluated with the observables $\mathbf{x}_i$ of the $i$th event. Since correlations among the observables are small ($< 10\%$), we take each $\mathcal{P}$ as the product of the PDFs for the separate variables.

The signal includes both CR and SCF signal components with the SCF fraction fixed in the fit to the value estimated from MC simulation. Both CR and SCF signals are used to measure the branching fraction and polarization. The PDF of the signal takes the form

$$\begin{aligned} P_{\mathrm{sig}} = {} & f_L(1 - g_L^{\mathrm{SCF}})\mathcal{P}_{\mathrm{CR},L} + f_L g_L^{\mathrm{SCF}} \mathcal{P}_{\mathrm{SCF},L} \\ & + f_T(1 - g_T^{\mathrm{SCF}})\mathcal{P}_{\mathrm{CR},T} + f_T g_T^{\mathrm{SCF}} \mathcal{P}_{\mathrm{SCF},T}, \end{aligned} \tag{3}$$

where $g_L^{\mathrm{SCF}}$ ($g_T^{\mathrm{SCF}}$) is the fraction of SCF in longitudinal (transverse) polarized signal events and $\mathcal{P}_{\mathrm{CR},L}$, $\mathcal{P}_{\mathrm{SCF},L}$ ($\mathcal{P}_{\mathrm{CR},T}$, $\mathcal{P}_{\mathrm{SCF},T}$) are the signal PDFs of CR and SCF signal components for longitudinal (transverse) polarization.

We determine the PDF parameters from Monte Carlo simulation for the signal and $B\bar{B}$ backgrounds and from off-resonance data for the continuum background.

We parametrize $m_{\mathrm{ES}}$ and $\Delta E$ using a Gaussian function with exponential tails [21] for the CR signal and charmless components, and using polynomials for all other components, except for the $m_{\mathrm{ES}}$ distribution for continuum events which is described by the ARGUS empirical phase space function [22] $x\sqrt{1 - x^2}\exp[-\xi(1 - x^2)]$, where $x \equiv 2m_{\mathrm{ES}}/\sqrt{s}$ and $\xi$ is a parameter. The $a_1$ mass is described by a relativistic Breit-Wigner function for the CR signal component, an asymmetric Gaussian plus a linear polynomial for the SCF signal component, and polynomials for the remaining components. The Fisher variable is parametrized with an asymmetric Gaussian plus a linear polynomial in all cases. The $\mathcal{H}$ variables are parametrized with a Gaussian plus a linear polynomial for the charm peaking

component and with a polynomial in all other cases. The parameters left free in the fit are the signal, continuum, and three $B\bar{B}$ component yields, and $f_L$. We also float some of the parameters of the continuum PDFs: the three parameters of the asymmetric Gaussian part of $\mathcal{F}$, and one parameter each for the $\mathcal{H}$, the $a_1$ masses, and $\Delta E$.

Large data samples of $B$ decays to charmed final states ($B^0 \to D^{*-} a_1^+$), which have similar topology to the signal, are used to verify the simulated resolutions in $m_{\rm ES}$ and $\Delta E$. Where the data samples reveal differences from the Monte Carlo, we shift or scale the resolution function used in the likelihood fits. Any bias in the fit, which arises mainly from neglecting the small correlations among the discriminating observables, is determined from a large set of simulated experiments for which the continuum background is generated from the PDFs, and into which we have embedded the expected number of $B\bar{B}$ background, signal, and SCF events chosen randomly from fully simulated Monte Carlo samples.

The fit results are presented in Table I. The detection efficiencies are calculated as the ratio of the number of signal MC events passing all the cuts to the total number generated. We compute the branching fraction by subtracting the fit bias from the measured yield, and dividing the result by the number of produced $B\bar{B}$ pairs times the product of the daughter branching fractions and the detection efficiency. We assume that the branching fractions of the $\Upsilon(4S)$ to $B^+B^-$ and $B^0\bar{B}^0$ are each 50%. The branching fraction and $f_L$ are corrected for the slightly different reconstruction efficiencies in longitudinal and transversal polarizations. The statistical uncertainty on the signal yield is taken as the change in the central value when the quantity $-2\ln\mathcal{L}$ increases by one unit from its minimum value. The significance is the square root of the difference between the value of $-2\ln\mathcal{L}$ (with systematic uncertainties included) for zero signal and the value at its minimum. In this calculation we have taken into account the fact that the floating $f_L$ parameter is not defined in the zero signal hypothesis.

TABLE I. Fitted signal yield and yield bias (in events), bias on $f_L$, detection efficiencies $\epsilon_L$ and $\epsilon_T$ for events with longitudinal and transversal polarization, respectively, significance $S$ (including systematic uncertainties), measured branching fraction $\mathcal{B}$, and fraction of longitudinal polarization $f_L$ with statistical and systematic uncertainties.

| | |
|---|---|
| Signal yield | $545 \pm 118$ |
| Signal yield bias | $+14$ |
| $f_L$ bias | $-0.06$ |
| $\epsilon_L$ (%) | 9.0 |
| $\epsilon_T$ (%) | 10.0 |
| $S$ ($\sigma$) | 5.0 |
| $\mathcal{B}$ ($\times 10^{-6}$) | $11.8 \pm 2.6 \pm 1.6$ |
| $f_L$ | $0.31 \pm 0.22 \pm 0.10$ |

Figure 1 shows the projections of $m_{\rm ES}$, $\Delta E$, the $a_1$ invariant mass, $\mathcal{F}$, and $\mathcal{H}$ for a subset of the data for which the ratio of the signal likelihood to the total likelihood (computed without using the variable plotted) exceeds a threshold that optimizes the sensitivity.

A systematic uncertainty of 38 events on the signal yield due to the PDF parametrization is estimated by varying the signal PDF parameters within their uncertainties, obtained through comparison of MC and data in control samples. The uncertainty from the fit bias (7 events) is taken as half the correction itself. Uncertainty from lack of knowledge of the $a_1$ meson parameters is 31 events. We vary the SCF fractions by their uncertainties and estimate a systematic uncertainty of 12 events. A systematic uncertainty of 19 events from possible contamination by $B^0 \to a_1(1260)^+ a_2(1320)^-$ background events is estimated with simulated MC experiments. The uncertainty due to cross feed between the signal and nonresonant backgrounds, evaluated with MC events, is 10 events. Uncertainties of 1.4% and 3.6% are associated with the track efficiency and particle identification, respectively. Differences between data and simulation for the $\cos\theta_T$ variable lead to a systematic uncertainty of 2.5%. Assuming that 20% of $a_1$ decays proceed through the $S$-wave $(\pi\pi)_\sigma$ channel [19], we estimate a systematic uncertainty of 6.8% from the difference in reconstruction efficiency between the $P$-wave $(\pi\pi)_\rho$ and $S$-wave components. The uncertainty in the total number of $B\bar{B}$ pairs in the data sample is 1.1%. The total systematic uncertainty, obtained by adding the individual terms in quadrature, is 12.9%.

The main systematic uncertainties on $f_L$ arise from the fit bias (0.03), the variation of PDF parameters (0.08), the $a_1$ parametrization (0.04), and the nonresonant background (0.02).

In conclusion, we have measured the branching fraction $\mathcal{B}(B^0 \to a_1^+ a_1^-) \times [\mathcal{B}(a_1^+ \to (3\pi)^+)]^2 = (11.8 \pm 2.6 \pm 1.6) \times 10^{-6}$ and the fraction of longitudinal polarization $f_L = 0.31 \pm 0.22 \pm 0.10$. Assuming that $\mathcal{B}(a_1^+ \to \pi^-\pi^+\pi^+)$ is equal to $\mathcal{B}(a_1^+ \to \pi^+\pi^0\pi^0)$, and that $\mathcal{B}(a_1^+ \to (3\pi)^+)$ is equal to 100% [19], we obtain $\mathcal{B}(B^0 \to a_1^+ a_1^-) = (47.3 \pm 10.5 \pm 6.3) \times 10^{-6}$. The decay mode is observed with a significance of $5.0\sigma$ including systematic uncertainties. The measured branching fraction and longitudinal polarization are in general agreement with the theoretical expectations in [2], while they disfavor those in [3].

We are grateful for the excellent luminosity and machine conditions provided by our PEP-II colleagues, and for the substantial dedicated effort from the computing organizations that support *BABAR*. The collaborating institutions wish to thank SLAC for its support and kind hospitality. This work is supported by DOE and NSF (USA), NSERC (Canada), CEA and CNRS-IN2P3 (France), BMBF and DFG (Germany), INFN (Italy), FOM (The Netherlands),

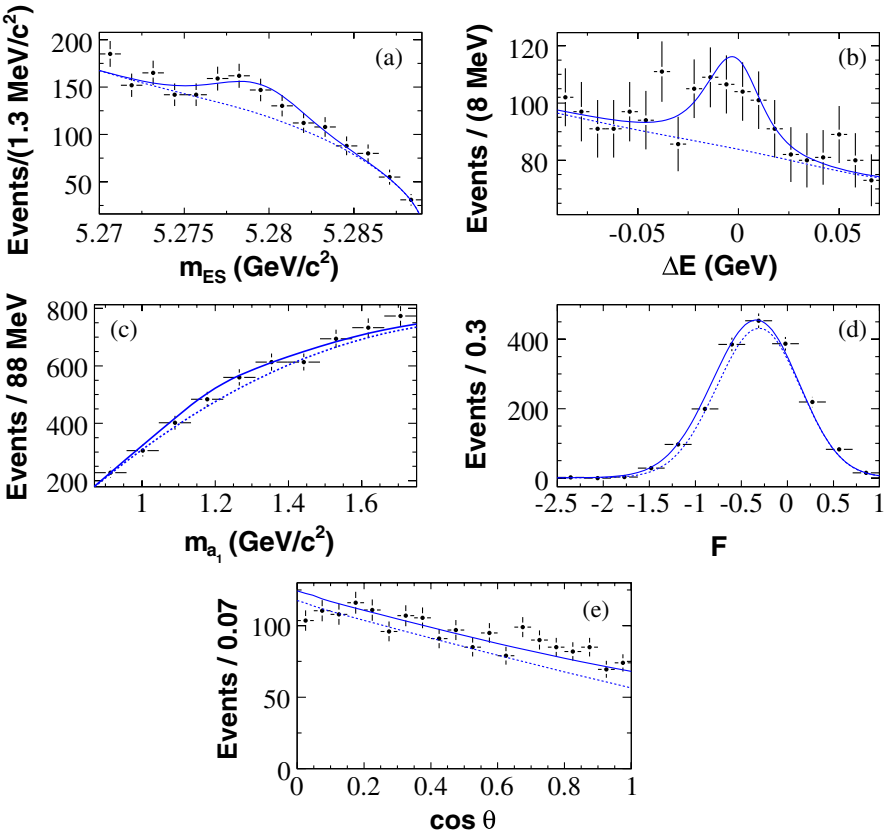


FIG. 1 (color online). Projections of (a) $m_{\rm ES}$, (b) $\Delta E$, (c) $a_1$ invariant mass (average of $m_{a_1^+}$ and $m_{a_1^-}$ is shown), (d) $\mathcal{F}$, and (e) $\mathcal{H} = |\cos\theta|$ (average of $|\cos\theta_{a_1^+}|$ and $|\cos\theta_{a_1^-}|$ is shown). Points with error bars (statistical only) represent the data, the solid line the full fit function, and the dashed line the background component. These plots are made with a requirement on the signal likelihood that selects 25%–40% of the signal and 2%–5% of the background.

NFR (Norway), MES (Russia), MEC (Spain), and STFC (United Kingdom). Individuals have received support from the Marie Curie EIF (European Union) and the A. P. Sloan Foundation.

[1] K.-C. Yang, Nucl. Phys. B, Proc. Suppl. **186**, 399 (2009).
[2] H.-Y. Cheng and K.-C. Yang, Phys. Rev. D **78**, 094001 (2008).
[3] G. Calderon *et al.*, Phys. Rev. D **76**, 094019 (2007).
[4] D. Bortoletto *et al.* (CLEO Collaboration), Phys. Rev. Lett. **62**, 2436 (1989).
[5] B. Aubert *et al.* (*BABAR* Collaboration), Phys. Rev. D **78**, 092008 (2008); K. F. Chen *et al.* (Belle Collaboration), Phys. Rev. Lett. **91**, 201801 (2003).
[6] A. V. Gritsan and J. G. Smith, "Polarization in *B* Decays", review in [19].
[7] A. Somov *et al.* (Belle Collaboration), Phys. Rev. Lett. **96**, 171801 (2006); B. Aubert *et al.* (*BABAR* Collaboration), Phys. Rev. D **76**, 052007 (2007); J. Zhang *et al.* (Belle Collaboration), Phys. Rev. Lett. **91**, 221801 (2003); B. Aubert *et al.* (*BABAR* Collaboration), Phys. Rev. Lett. **102**, 141802 (2009).
[8] B. Aubert *et al.* (*BABAR* Collaboration), Phys. Rev. D **79**, 052005 (2009).
[9] B. Aubert *et al.* (*BABAR* Collaboration), Phys. Rev. Lett. **98**, 051801 (2007).
[10] A. L. Kagan, Phys. Lett. B **601**, 151 (2004); C. W. Bauer *et al.*, Phys. Rev. D **70**, 054015 (2004); P. Colangelo, F. De Fazio, and T. N. Pham, Phys. Lett. B **597**, 291 (2004); M. Ladisa *et al.*, Phys. Rev. D **70**, 114025 (2004); H. Y. Cheng, C. K. Chua, and A. Soni, Phys. Rev. D **71**, 014030 (2005); H. N. Li and S. Mishima, Phys. Rev. D **71**, 054025 (2005); C. H. Chen *et al.*, Phys. Rev. D **72**, 054011 (2005); M. Beneke *et al.*, Nucl. Phys. **B774**, 64 (2007).
[11] A. K. Giri and R. Mohanta, Phys. Rev. D **69**, 014008 (2004); E. Alvarez *et al.*, Phys. Rev. D **70**, 115014 (2004); P. K. Das and K. C. Yang, Phys. Rev. D **71**, 094002 (2005); C. H. Chen and C. Q. Geng, Phys. Rev. D **71**, 115004 (2005); Y. D. Yang, R. M. Wang, and G. R. Lu, Phys. Rev. D **72**, 015009 (2005); C. S. Hunger *et al.*,

Phys. Rev. D **73**, 034026 (2006); C. H. Chen and C. Q. Geng, Phys. Rev. D **75**, 054010 (2007).

[12] $a_1$ will be used to indicate the $a_1(1260)$ meson.

[13] Charge conjugate decay modes are implied unless specifically stated.

[14] B. Aubert *et al.* (*BABAR* Collaboration), Phys. Rev. Lett. **97**, 051802 (2006).

[15] B. Aubert *et al.* (*BABAR* Collaboration), Nucl. Instrum. Methods Phys. Res., Sect. A **479**, 1 (2002).

[16] PEP-II Conceptual Design Report, Report No. SLAC-R-418, 1993.

[17] B. Aubert *et al.* (*BABAR* Collaboration), Phys. Rev. D **70**, 032006 (2004).

[18] The *BABAR* detector MC simulation is based on GEANT 4: S. Agostinelli *et al.*, Nucl. Instrum. Methods Phys. Res., Sect. A **506**, 250 (2003).

[19] C. Amsler *et al.* (Particle Data Group), Phys. Lett. B **667**, 1 (2008).

[20] EvtGen particle decay simulation package, D. J. Lange, Nucl. Instrum. Methods Phys. Res., Sect. A **462**, 152 (2001).

[21] We use the following function:

$$f(x) = \exp\left(\frac{-(x-\mu)^2}{2\sigma_{L,R}^2 + \alpha_{L,R}(x-\mu)^2}\right),$$

where $\mu$ is the peak position of the distribution, $\sigma_{L,R}$ are the left and right widths, and $\alpha_{L,R}$ are the left and right tail parameters.

[22] H. Albrecht *et al.* (ARGUS Collaboration), Phys. Lett. B **241**, 278 (1990).